The Nature of the Hydrogen Bond to Water in the Gas Phase

A. C. Legon
Department of Chemistry, University of Exeter, Stocker Road, Exeter EX4 4QD
D. J. Millen
Christopher Ingold Laboratories, Department of Chemistry, University College London, 20 Gordon Street, London WC1H 0AJ

1 Introduction

One of the reasons for investigating the hydrogen bond is the central rôle played by this weak interaction in biological structures and processes, in the chemistry of aqueous solutions and, of course, in determining the properties of water. It is necessary in pure water that the water molecule acts both as a proton donor and a proton acceptor in forming a hydrogen-bond interaction. The same is true, for example, of hydrogen fluoride molecules in liquid hydrogen fluoride or of ammonia molecules in liquid ammonia. But what happens in aqueous solutions of these substances? Do the water molecules then act as the proton acceptor or the proton donor? Many other important questions about such mixtures also arise but are difficult to answer because of the complications associated with the liquid phase. A simpler approach is to consider, for example, the interaction of a water molecule and a hydrogen fluoride molecule in the gas phase at low pressure and therefore in the isolated heterodimer. In fact, the particular heterodimer of H_2O and HF has been investigated[1-7] in great detail *via* its rotational spectrum and consequently more is known of its properties in isolation than any other dimer. In parallel, a number of other gas-phase dimers involving water either as the proton acceptor or the proton donor have been examined. Examples in which water is the proton acceptor $H_2O\cdots HX$ include:[1,12]

$$H_2O\cdots HF,\ H_2O\cdots HCl,\ H_2O\cdots HBr,\ H_2O\cdots HCN,\ H_2O\cdots HCCH,\ H_2O\cdots H_2O$$

while among those in which water is the donor are[13,14]

$$H_3N\cdots H_2O,\ N_2\cdots H_2O,\ H_2O\cdots H_2O$$

It is timely to review the conclusions reached about hydrogen bonding by the water molecule in this range of dimers in a general way and in the archetypal dimer $H_2O\cdots HF$ in detail.

We consider first which questions about the hydrogen-bond interaction are important to answer. The first of these is: can we predict under which circumstances H_2O will act as a proton donor and under which circumstances it will act as an acceptor. We shall show later that it is possible to assign to a molecule numbers E and N, called the gas-phase electrophilicity and nucleophilicity, respectively, that measure the propensity for that molecule to act as a donor or an acceptor. The product of E and N then provides a criterion for deciding, for example, whether $H_2O\cdots HF$ or $HF\cdots HOH$ is the favoured isomer of the dimer of H_2O and HF. Thus, if $E_{H_2O}N_{HF} < E_{HF}N_{H_2O}$ the lower energy form will be $H_2O\cdots HF$. In this case, the inequality is large and the conclusion is in accord with chemical intuition. For the dimer of H_2O and HCN, on the other hand, the favoured isomer is not self-evident and this is reflected in a near-equality of the two terms.

Given that the form $H_2O\cdots HF$ of the water–hydrogen fluoride dimer in which H_2O is the proton acceptor is favoured, the second question concerns the configuration at the oxygen atom: is it planar or pyramidal, *i.e.* does $H_2O\cdots HF$ have C_{2v} or C_s symmetry? This question, which does not have a simple answer, will be discussed in detail. We shall show that the angular geometry of a dimer $B\cdots HX$ is determined, in good approximation, by the variation of the electrostatic potential around B. Hence, in so far as angular geometries are concerned, interest will centre on dimers $H_2O\cdots HX$ rather than dimers $B\cdots H_2O$ since only in the former does H_2O control the geometry. The third question is simply: is the description $H_2O\cdots HX$ or $H_3O^+\cdots X^-$ appropriate? We shall show from simple arguments that in isolation $H_2O\cdots HX$ is overwhelmingly favoured for X = F, Cl, Br, CN, and we can therefore expect to observe this form spectroscopically in the vapour phase. Only under extreme conditions, such as exist in an electrical discharge, can the ion H_3O^+ be observed in the gas phase but, of course, the concept of ions H_3O^+ and X^- is familiar in discussions of aqueous solutions of mineral acids where solvation plays a controlling rôle. Hydrogen-bonded ion pairs do exist in the gas-phase, however. When H_2O in $H_2O\cdots HX$ is replaced by the stronger nucleophile $(CH_3)_3N$, the description $(CH_3)_3N^+H\cdots X^-$ can become more appropriate, as in the case X = Br.

Other important questions about $H_2O\cdots HX$ are concerned with the distance $r(O\cdots X)$ and its dependence on H/D substitution, the exact position of the hydrogen-bond proton (*i.e.* how much does HX extend on dimer formation), the energy required to extend the hydrogen bond infinitesimally and infinitely, and the energy required to bend the hydrogen bond. Finally, we shall address the question of what electrical perturbations of the subunits accompany formation of $H_2O\cdots HX$.

2 When Does Water Act as a Proton Acceptor and When Does it Act as a Proton Donor?

The intermolecular stretching force constant k_σ for a weakly bound dimer is available on the basis of a very simple model[15] from the centrifugal distortion constant D_J(or Δ_J) which is in

A. C. Legon is Professor of Physical Chemistry in the University of Exeter. He was educated at the Coopers' Company School in Bow, London and at University College London. His recent research interests include systematic investigations of hydrogen-bonded (and other weakly bound) complexes by microwave and infrared spectroscopy of pulsed, supersonic jets. He was Tilden Lecturer and Medallist of the Royal Society of Chemistry for 1989—90.

D. J. Millen began research at University College London under the supervision of Dr. H. G. Poole and Sir Christopher Ingold. In 1950 he was a Commonwealth Fund Fellow at Harvard working with Professor Bright Wilson. He returned to UCL and was appointed Reader in 1959 and Professor in 1964. In 1967 he was Nyholm Lecturer and Medallist of the Royal Society of Chemistry and President of its Education Division for 1979—81. He has had a long-standing research interest in hydrogen bonding, first in Raman spectroscopy of some solid hydrates, then in infrared spectroscopy of gas-phase dimers, and more recently in microwave spectroscopy of such dimers.

turn straightforwardly determined from the rotational spectrum of the dimer. The model assumes that each of the subunits in B···HX is itself rigid and in the quadratic approximation D_J depends only on the hydrogen-bond stretching force constant. As a result, k_σ is available for a wide range of hydrogen-bonded dimers and by systematically varying first B and then HX it has been possible to recognize[16] a simple pattern among the k_σ values, namely that a number N, called the limiting gas-phase nucleophilicity, can be assigned to B and that a number E, correspondingly, the electrophilicity can be assigned to HX such that for a given B···HX, k_σ is related to N and E by

$$k_\sigma = cNE \quad (1)$$

Table 1 Nucleophilicities N and electrophilicities E for selected molecules

Molecule	N	E
H_2O	10.0	5.0
HF	4.8	10.0
HCl	3.1	5.0
HCN	7.3	4.25
HCCH	5.1	2.4

where $c = 0.25$ Nm^{-1}. Table 1 shows a selection of N and E values so assigned. We now consider the relative stability of the two isomers H_2O···HX and HX···HOH that can be formed by water and a molecule HX. It is assumed that if the product $N_{H_2O}E_{HX} > N_{HX}E_{H_2O}$, the isomer H_2O···HX will be more stable than the isomer HX···HOH, and *vice versa*. For dimers B···HF where both k_σ and dissociation energy D_0 are known, there is a good correlation between these quantities, suggesting that the order of k_σ values may well parallel the order of D_0. In Table 2, we compare the products $N_{H_2O}E_{HX}$ and $N_{HX}E_{H_2O}$ for a series of dimers H_2O···HX and HX···H_2O, where HX = HF, HCl, HCN, HCCH, and H_2O. We note that for the first two members of the series the form H_2O···HX is strongly favoured. Although the isomer H_2O···HX is slightly favoured for X = CN, the two isomers H_2O···HCCH and HCCH···HOH appear to be of similar stability. In fact, in experiments using supersonically expanded mixtures of H_2O and HX in argon only the isomers H_2O···HX have so far been observed for all groups X mentioned above. Of course, in these experiments the effective temperature of the expanded gas is very low and only the lowest energy isomer will be observed even when the energy difference is very small. We conclude that, because the N value for water is significantly larger than its E value, dimers of the type H_2O···HX predominate in the observations made so far. Nevertheless if N_{HX} is large enough compared with E_{HX} (*e.g.* as in NH_3) the form HX···HOH will be observed in supersonic expansions (*e.g.* H_3N···HOH[13]).

Table 2 Values of N_{H_2O} E_{HX} and N_{HX} E_{H_2O} for dimers H_2O···HX and HX···HOH

HX	HF	HCl	HCN	HCCH	H_2O
N_{H_2O} E_{HX}	100.0	50.0	42.4	24.0	50.0
$N_{HX}E_{H_2O}$	24.0	15.6	36.4	25.6	50.0

3 The Configuration at Oxygen in H_2O···HF: Planar or Pyramidal?

Traditionally, rotational spectroscopy has been a powerful method of determining the geometry of a molecule in isolation and relies on the fact that the observed transition frequencies lead to moments of inertia and these depend on the distribution of mass within the molecule *i.e.* on the positions of the atoms. The detailed examination of the rotational spectra obtained from numerous isotopomers of H_2O···HF shows that the order of the nuclei is unambiguously as indicated.[1] The contribution from the hydrogen atoms to the moments of inertia is however necessarily small in this case, and it proves not to be possible on the basis of moments of inertia to distinguish between a geometry having a pyramidal configuration at oxygen (*i.e.* one of C_s symmetry) and one having a planar arrangement at oxygen (*i.e.* with C_{2v} symmetry). The difficulty arises because the observed moments of inertia are not equilibrium values and are significantly modified by the zero-point motion of the molecule. If the three principal equilibrium moments of inertia I_a^e, I_b^e, and I_c^e, were available the conditions $I_c^e \leqslant I_a^e + I_b^e$, would provide a criterion of planarity (=) or otherwise (<). When zero-point moments of inertia are used, however, the equality does not strictly hold, even for a molecule with a planar equilibrium geometry.

To make further progress with zero-point quantities, we must examine the variation of the moments of inertia with vibrational excitation of the mode $\nu_{\beta(o)}$ that takes the planar molecule out of the plane or, if the equilibrium geometry is non-planar, that takes the molecule towards the plane. A schematic diagram of this motion is included in Figure 1, where for convenience a planar arrangement is assumed. The motion can in fact be defined in terms of a single vibrational coordinate θ (see Figure 2) which under the above assumption is zero in the planar form.

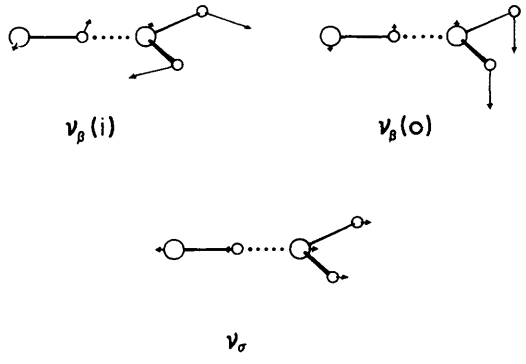

Figure 1 Schematic representation of the three lowest energy hydrogen bond modes in H_2O···HF.

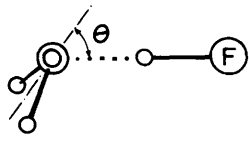

Figure 2 Definition of the angle θ in H_2O···HF.

Depending on the equilibrium conformation of H_2O···HF, we can envisage three general forms for the variation of the potential energy of the molecule as θ is changed from zero. These are shown in Figure 3. When the equilibrium geometry is planar ($\theta_e = 0$) the vibrational energy levels [$v_{\beta(o)}$] associated with the mode are well behaved (Figure 3a) and the vibrational probabilities are as shown. Of course, states with even v have a maximum probability at $\theta = 0$ while those of odd v have zero probability there. If a small barrier is now introduced at $\theta = 0$, its effect is to perturb even states disproportionately so that the $v = 0$ and $v = 1$ levels move closer together while $v = 1$ and $v = 2$ diverge. The result for a barrier that is lower than the $v = 2$ level is shown in Figure 3b. As the barrier height is increased these effects increase very rapidly and the $v = 0$ and 1 levels soon become effectively degenerate, as illustrated in Figure 3c where the barrier is so high that the $v = 2$ and 3 levels are also degenerate. Molecules in the $v = 0,1$ pair of degenerate levels are then

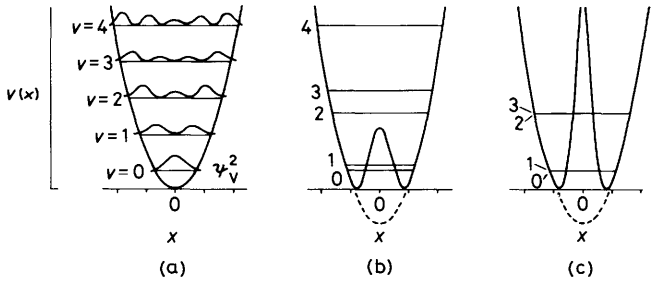

Figure 3 (a) Potential energy function, vibrational energy levels, and probability distributions of a harmonic oscillator. (b) As a barrier is introduced at $x = 0$, the vibrational energy levels begin to draw together in pairs. (c) In the limit of a high barrier, the pairs have become degenerate.

permanently pyramidal. For a molecule with a potential energy function $V(\theta)$ like that in Figure 3b, the zero-point state can be described as *effectively* planar because the vibrational wavefunction has C_{2v} symmetry but the equilibrium geometry of the molecule nevertheless has C_s symmetry, *i.e.* is pyramidal. It is possible to assign $H_2O\cdots HF$ to one of the types in Figure 3 by examining the rotational spectrum in several of the vibrational states $v_{\beta(o)} = 0,1,2\ldots$.

In the case of $H_2O\cdots HF$, it is possible to show that the potential energy function $V(\theta)$ is not of the type shown in Figure 3c by arguments based on a nuclear spin statistical weight effect in the rotational spectrum.[1] Briefly, the effect in $H_2O\cdots HF$ is just as observed in the dihydrogen molecule, where some rotational energy levels have a weight of 3 (*ortho*-H_2) and the others have a weight of 1 (*para*-H_2). This establishes that, as for the dihydrogen molecule, a twofold rotation exchanges a pair of equivalent protons in $H_2O\cdots HF$. Thus, a rigidly pyramidal molecule of the type in which the lowest pair of vibrational energy levels are degenerate, as in the example of Figure 3c, is excluded because it has no C_2 axis and no equivalent hydrogen atoms under a twofold rotation. It remains to decide whether $H_2O\cdots HF$ is governed by a function of the type in Figure 3a or 3b, both of which would lead to the observed nuclear spin statistical weight effects. This can be achieved by considering the variation of the observed moments of inertia with the vibrational quantum number $v_{\beta(o)}$. The observed quantity is an average over the vibrational state in question and will thus reflect even a small perturbation of the wavefunction arising from a small potential energy barrier at the planar molecule. When the barrier is zero, the effective moments of inertia I_v will vary smoothly with v, but when $V(\theta)$ has a double minimum the relatively larger perturbation of v even states leads to a zig-zag behaviour of I_v when plotted against v. $H_2O\cdots HF$ does indeed exhibit this effect[2] and therefore the barrier at $\theta = 0$ cannot be zero. It has already been shown, however, that the barrier cannot be large. Hence $H_2O\cdots HF$ corresponds to the case shown in Figure 3b. Relative intensity measurements of a given rotational transition in the $v_{\beta(o)} = 0,1$, and 2 states lead[2] to the vibrational spacings of 64(10) and 203(35) cm^{-1} for $v_{\beta(o)} = 1 \leftarrow 0$ and $2 \leftarrow 1$ respectively, thus confirming the irregular vibrational spacing and the qualitative form of the potential energy function. In fact, the quantitative form of $V(\theta)$ has also been determined,[2] essentially by fitting the variation of I_v with $v_{\beta(o)}$ and the observed vibrational separations. The result is shown in Figure 4 where it is seen that the barrier is indeed low at 1.5 kJ mol^{-1}, which should be compared with the dissociation energy D_0 (34 kJ mol^{-1}) of the complex.

4 The Configuration at Oxygen in $H_2O\cdots HF$: Can it be Predicted by a Simple Model?

The experimental result that $V(\theta)$ for $H_2O\cdots HF$ is a double-minimum potential energy function (see Figure 4) with the equilibrium angle $\theta_e = 46(8)°$ has important consequences for

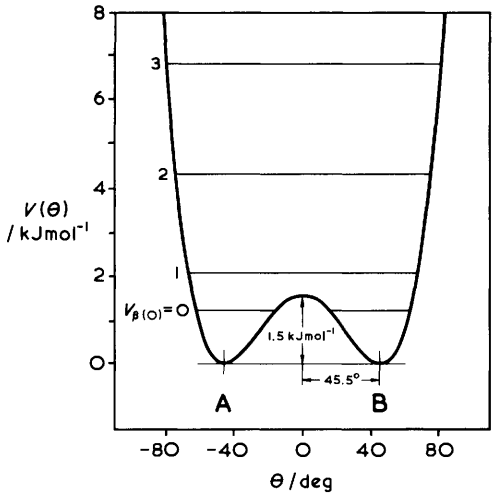

Figure 4 The experimentally determined one-dimensional potential energy function $V(\theta)$ *versus* θ for the hydrogen-bonded dimer $H_2O\cdots HF$. See Figure 2 for the definition of the angle θ.

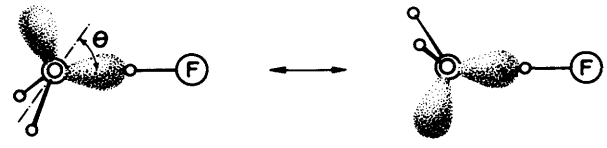

Figure 5 A simple model that accounts qualitatively for the form of the observed potential energy function $V(\theta)$ in $H_2O\cdots HF$. In each of the two equivalent equilibrium conformations, the HF molecule lies along the axis of a non-bonding electron pair (drawn schematically) on the oxygen atom.

modelling the hydrogen bond. First, it strongly suggests a very simple electrostatic model[17] in which the HF molecule lies at equilibrium along the axis of a non-bonding electron pair on the oxygen atom, as illustrated in Figure 5. The assumption is that the electric charge distribution of H_2O is not greatly perturbed by the proximity of the HF molecule. The variation of the θ_e along the series $B\cdots HF$, where B = 2,5-dihydrofuran, oxetane, and oxirane, from 48.5° through 57.9° to 71.8° strongly supports the simple n-pair model because such an increase is consistent with opening of the inter-lone-pair angle as the angle COC decreases along with the series of molecules B.[18] Secondly, the quantitative form of $V(\theta)$ for $H_2O\cdots HF$ provides a critical test for theoretical modelling of the angular dependence of the hydrogen-bond interaction, especially because of the small number of electrons in this entirely first-row dimer. In fact, it is interesting to record that the variation with θ of the electrostatic potential energy of a test point-charge at a fixed distance from the oxygen atom leads to a curve of shape closely similar to that in Figure 4. The result when the point charge is $+0.54\,e$ and the distance is the experimental $r(O\cdots H)$ is shown in Figure 6.[19] The potential energy barrier of ≈ 0.5 kJ mol^{-1} is in reasonable agreement with the observed value. The reason for choosing a charge of $+0.54\,e$ is that the electric charge distribution of HF can be represented in good approximation simply by $0.54\,e$ on H and $-0.54\,e$ on F. Consequently, if the F end is ignored in making a zeroth approximation to the HF molecule, the interaction energy of H_2O and HF is just the electrostatic potential energy shown in Figure 6. At the next level of approximation, the charge on F can be included and HF considered as an extended electric dipole. When such a charge distribution is rolled around water, the variation of $V(\theta)$ is as shown in Figure 6, where the component electrostatic energies of the charges on H and F are also given.[19] We note that θ_e is now very close to one half of the tetrahedral angle, further reinforcing the non-bonding pair interpretation, while the barrier height is 3.5 kJ mol^{-1}.

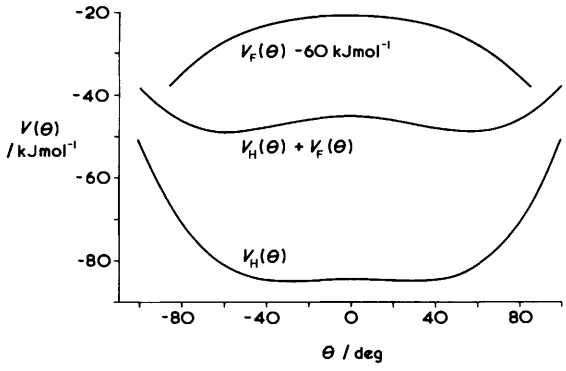

Figure 6 Variation of the electrostatic potential energy with angle θ for a point charge + 0.54 e at the experimental O···H distance from O in H_2O···HF [$V_H(\theta)$], for a point charge − 0.54 e at the experimental distance O···F from O in H_2O···HF [$V_F(\theta)$], and the sum $V_H(\theta) + V_F(\theta)$. See text for discussion and Figure 2 for the definition of the angle θ.

An even better description of the interaction between the H_2O and HF molecules uses a complete description of the electric charge distribution of each and was developed by Buckingham and Fowler.[20] In fact the curves referred to in Figure 6 rely on the more complete description of the electrostatic charge distribution for water given by these authors. Their method is to represent accurately a good *ab initio* SCF charge distribution of the molecule by the so-called Distributed Multipole Analysis (DMA) which places point charges, dipoles, and quadrupoles on each atom. The global minimum found in the electrostatic energy of interaction as a function of the relative angular orientation of the two component molecules at an appropriate van der Waals distance has been found to give excellent agreement with the experimental angular geometry for a wide range of dimers, whether hydrogen-bonded or other weakly bound systems. In fact, the reason for choosing in the above discussion HF as an extended electric dipole having charges ± 0.54 e stems from the Buckingham–Fowler DMA of HF in which the point charges dominate the description. Of course, a point-charge model for both H_2O and HF would have advantages from the view point of simplicity and physical insight. Such a model has in fact been developed for a small number of molecules B, including H_2O.

In this simplified model,[21] a point-charge representation of the electric charge distribution of B is used together with the above-mentioned extended point dipole model of HF. In particular it has been shown that to obtain agreement with experiment (where available) and with calculations based on the full Buckingham–Fowler model, it is necessary to place only small fractional electronic charges at physically reasonable distances along the directions usually associated with non-bonding electron pairs. The definition of the fractional electronic charges δ, and their distances r from oxygen at the required angle of $\alpha = 54°$ are shown in Figure 7. The point charges on H and O are 0.401 e and − 0.724 e, as in the published DMA for H_2O but with 2 × δ

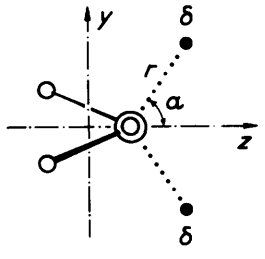

Figure 7 Definition of the fractional charge δ, its distance r from the O atom and the angle α for a simple point-charge model of H_2O. See text for discussion.

(= 2 × − 0.039 e) removed from the charge on O. Such a model of H_2O gives the correct dependence of $V(\theta)$ on θ with a potential energy barrier of magnitude ≈ 3.5 kJ mol^{-1} and $\theta_e = 45°$. Parallels with the valence-shell-electron-pair repulsion model of Gillespie and Nyholm[22] and with the partial localization of electron density along non-bonding pair directions discussed by Bader *et al.*[23] are obvious. Thus this model accounts for the pyramidal configuration at oxygen in H_2O···HF by placing small fractional electron charges in the positions usually attributed to non-bonding pairs while the Buckingham–Fowler model achieves the same result with the aid of a point electric quadrupole on oxygen.

5 How Does the Configuration at Oxygen Change Along the Series H_2O···HX, Where X = F, Cl, Br, or CN?

It is clear from the discussion in Section 4 that the angular geometry of a hydrogen-bonded dimer like H_2O···HF is determined largely by the variation of the electrostatic potential with angle at a given distance in the vicinity of B (*i.e.* H_2O). Presumably, as the distance from H_2O increases the double minimum apparent in the potential function $V(\theta)$ (see, for example, Figure 6) begins to disappear. This is shown clearly in Figure 8 where the electrostatic potential energy of the HF molecule described as an extended dipole + 0.54 e and − 0.54 e is plotted as a function of angle θ for various distances r(O···H). Even for distances as small as 2.0—2.5Å the function has only a single minimum and therefore a dimer H_2O···HX in which the r(O···H) distance is of this magnitude would have a planar equilibrium geometry of C_{2v} symmetry. Distances r(O···H) in this range have been observed[8–10] in H_2O···HCl, H_2O···HBr, and H_2O···HCN. Consequently, it seems possible that some of these dimers have the C_{2v} equilibrium arrangement. The experimental investigations[8–10] made on this series certainly indicate a low barrier to the planar form in each case, but have so far been unable to distinguish between the effectively planar C_s molecule with a low barrier and the strictly planar C_{2v} equilibrium geometry.

6 What is the Length of the Hydrogen Bond and Where is the Proton in H_2O···HX?

The questions of most interest about the length of the hydrogen bond in H_2O···HX are:

(i) What is the distance between the heavy atoms O and X?
(ii) Has the HX bond lengthened significantly on formation of H_2O···HX?
(iii) Are the O, H, X nuclei collinear at equilibrium?

The first of these questions is the easiest to answer from the observed ground-state moments of inertia of H_2O···HX. This is achieved simply by assuming unchanged H_2O and HX geometries (see below) and an effectively planar arrangement in the zero-point state. In fact, small changes in the OH and HX distances contribute negligibly to the dimer moments of inertia. The distance r(O···X) is then varied until the ground-state rotational constants are reproduced. The results for X = F, Cl, Br, and CN are given in Table 3.[1,8–10] Another point of interest is the effect on r(B···X) of a change from a hydrogen to a deuterium bond in B···HX. A wide range of B···H(D)X has been investigated (including B = H_2O), a generalization identified, and a model proposed to account for the observed effects.[24]

A concomitant of the insensitivity of the calculated rotational constants to the distance r_{HX} is that the latter quantity is not available from the former. But, in the dimers B···HF, the H,F nuclear spin–nuclear spin coupling constant, which is proportional to the zero-point average of r_{HF}^{-3} carries the required information. Unfortunately, this information is convoluted in the coupling constant with the effects of the angular motion of the HF subunit in the dimer which makes the predominant

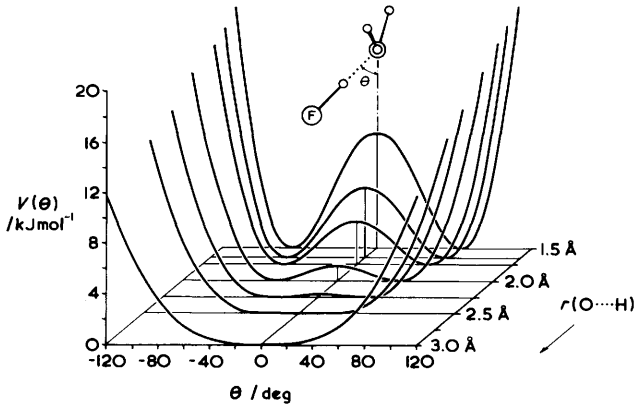

Figure 8 Calculated variation of the electrostatic potential energy $V(\theta)$ of the HF molecule with the angle θ in the $H_2O\cdots HF$. The HF molecule, treated as a simple extended electric dipole with charges $+0.54e$ and $-0.54e$ on the H and F atoms, makes an angle θ with the bisector of the HOH angle and lies in the plane of the non-bonding electron pairs on O. Each curve refers to a different distance r of the H atom of HF from O.

Table 3 Observed $r(O\cdots X)$ in $H_2O\cdots HX$, where X = F, Cl, Br, or CN

$H_2O\cdots HX$	$r(O\cdots X)$/Å
F	2.662[a]
Cl	3.215[b]
Br	3.411[c]
CN	3.139[d]

[a]Ref. 1. [b]Ref. 8. [c]Ref. 9. [d]Ref. 10.

contribution to the zero-point average. However, a deconvolution is possible if the isotopomer $B\cdots DF$ is examined and the deuterium nuclear quadrupole coupling constant is available. Details of the approach are given elsewhere[25] for a series of dimers $B\cdots H(D)F$. The result for $H_2O\cdots HF$ is a lengthening $\delta r = 0.017$ Å of the HF bond which is in excellent agreement with the value from a sophisticated *ab initio* SCF calculation that includes electron correlation *via* second and third order Møller-Plesset perturbation theory.[26] A very simple electrostatic model[27] put forward recently for the HF bond lengthening leads to a value of 0.020 Å which is in satisfactory agreement with both experiment and the *ab initio* value. We conclude, therefore, that the contribution of the valence-bond structure $H_2O\cdots HF$ to the description of the dimer is preponderant while that of $H_3O^+\cdots F^-$ is very small.

The small contribution of $H_3O^+\cdots F^-$ is in agreement with some conclusions based on simple thermodynamic arguments applied to the process

$$H_2O\cdots HX = H_3O^+\cdots X^- \quad (2)$$

If it assumed that $r(O\cdots X)$ is unchanged, ΔE_2 can be estimated from energy changes for the following reactions:

$$H_2O\cdots HX = H_2O + HX \quad (3)$$

$$H_2O + H^+ = H_3O^+ \quad (4)$$

$$HX = H^+ + X^- \quad (5)$$

$$H_3O^+ + X^- = H_3O^+\cdots X^- \quad (6)$$

since $\Delta E_2 = \sum_{i=3}^{6} \Delta E_i$ and the ΔE_i are readily estimated. Thus, $\Delta E_3 \approx D_o$, the zero-point dissociation energy, which has been measured[7] for $H_2O\cdots HF$ and whose value for other X can be estimated by assuming that the D_0 values scale according to the known k_o. ΔE_4 can be approximated as minus the proton affinity

Table 4 Estimates of the energy change ΔE_2 for the reaction $H_2O\cdots HX = H_3O^+\cdots X^-$, where X = F, Cl, Br, or CN

	ΔE_i/kJ mol^{-1}[a]					
$H_2O\cdots HX$	$i=3$	4	5	6	2[c]	M_{eff}[b]
F	34.3[d]	−691.6	1554	−521.9	374.8	1.718
Cl	17.1[e]	−691.6	1394	−432.1	287.4	1.665
Br	14.4[e]	−691.6	1354	−407.3	269.5	1.662
CN	14.6[e]	−691.6	1461	−440.7	343.3	1.779

[a]See text and ref. 28 for the origin of the various ΔE_i values. The subscript i refers to equations 3—6. [b]M_{eff} is the effective Madelung constant. It is the number by which ΔE_6 must be multiplied to make ΔE_2 zero. The smallest possible value for a Madelung constant is 1.748 for a face-centred cubic lattice. Hence, the solid H_2O + HX where X = F, Cl, and Br will be ionic but H_2O + HCN is unlikely to be. [c]$\Delta E_2 = \sum_{i=3}^{6} \Delta E_i$ (see text). [d]Experimental value of D_0 from ref. 7. [e]Estimated values assuming $k_o^X/k_o^F = D_0^X/D_0^F$ holds for the series $H_2O\cdots HX$.

of H_2O. ΔE_5 is well known and ΔE_6 is just the Coulombic energy gained when the ions are brought to the appropriate distance apart. The small repulsive contribution to ΔE_6 can be ignored for present purposes. The results of this procedure are summarized in Table 4. For each X, it is clear that ΔE_2 is large and positive and we can conclude that the form $H_2O\cdots HX$ is predominant in each case in the gas phase. But the situation is quite different in condensed phases. For the solid phase, the calculation of ΔE_2 would require the use of ΔE_6 but multiplied by the appropriate Madelung constant. It is convenient therefore to calculate an effective value of the Madelung constant M_{eff} which makes ΔE_2 zero. These values are shown in the final column of Table 4. We note that for X = Cl and Br M_{eff} is considerably less than the typical value 1.748 for the rock salt lattice and so it can be understood why these mineral acid monohydrates have ionic crystal structures. On the other hand, for $H_3\dot{O}\cdots\bar{C}N$, M_{eff} is larger than the typical value and suggests that, in the solid state, hydrogen cyanide monohydrate would not be ionic. In aqueous solution, solvation energies replace lattice energies in these considerations but, if it can be assumed that the solvation energy of $H_3\dot{O}$ is similar to that of an alkali metal cation for which the solvation enthalpies are closely similar to the appropriate lattice energy, it is not unexpected that HCl and HBr are strong acids. It is worth noting at this point that the ion-pair from $\dot{B}H\cdots\bar{X}$ can have lower energy than the simple hydrogen bonded dimer $B\cdots HX$ even in the gas phase if the acceptor molecule B has a sufficiently large proton affinity and the donor molecular HX has a suitably small energy for dissociation in the manner of equation 5. Thus it has been demonstrated[28] by investigation of its rotational spectrum that trimethylammonium bromide is better described in the gas phase as the ion pair $(CH_3)_3\dot{N}H\cdots\bar{B}r$ than as the simple hydrogen-bonded dimer $(CH_3)_3N\cdots HBr$.

The third question posed above, which concerns the collinearity of the O, H, and X nuclei at equilibrium, is difficult to answer through rotational spectroscopy because of the insensitivity of rotational constants to the exact position of the H atom. On the other hand, the electrostatic model of Buckingham and Fowler[20] finds a small deviation from linearity in $H_2O\cdots HF$, as illustrated in Figure 9, in the direction that would result from a

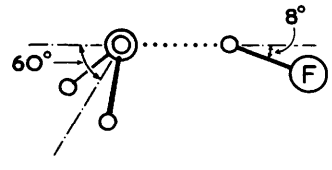

Figure 9 The angular geometry of the $H_2O\cdots HF$ dimer predicted by the Buckingham–Fowler electrostatic model. Note that the hydrogen bond is predicted to be slightly bent in the direction that would favour a secondary $H\cdots F$ interaction and that the angle $O\cdots H-F$ is 172°.

secondary hydrogen bond interaction. In fact, recently some experimental evidence for a similar degree of bending has been presented for the vinyl fluoride–hydrogen chloride dimer.[29] Reasons why only small deviations from linearity are found in isolated hydrogen-bonded dimers have been discussed in the light of the hydrogen-bond bending force constants[5] and the electrostatic model[19] of $H_2O\cdots HF$.

7 How Strong is the Hydrogen Bond in $H_2O\cdots HF$?

There are, of course, several ways to measure the strength of a hydrogen bond. We might first ask how easily is the hydrogen bond stretched (radial deformation), either infinitesimally or infinitely, and then how easily is the bond bent (angular deformation).

7.1 How Difficult is it to Deform $H_2O\cdots HF$ Radially?

The ease of radial deformation of $H_2O\cdots HF$ can be measured in two ways. First, the quadratic force constant k_σ associated with the hydrogen-bond stretching mode ν_σ gives, *via* the usual expression $\frac{1}{2}k_\sigma\delta r^2$, the energy required for a unit infinitesimal extension δr along the dissociation coordinate from equilibrium. Second, the dissociation energy D_0 defines the energy necessary for an infinite extension along the same coordinate to give the separate components H_2O and HF. Both of these quantities can in fact be obtained from measurements of the rotational spectrum in the case of $H_2O\cdots HF$.[7,16]

Table 5 Intermolecular stretching force constants k_σ for dimers $H_2O\cdots HX$

Dimer	k_σ/Nm^{-1}
$H_2O\cdots HF$	24.9[a]
$H_2O\cdots HCl$	12.5[a]
$H_2O\cdots HCN$	11.1[a]
$H_2O\cdots H_2O$	11.7[b]
$H_2O\cdots HCCH$	6.5[a]

[a]For a convenient compilation, see ref. 16. [b]Ref. 12.

The determination of k_σ from the centrifugal distortion constants D_J (or Δ_J) has already been mentioned in Section 2. Values of k_σ determined for $H_2O\cdots HX$, where X = F, Cl, CN, and Br, are recorded in Table 5. The quantity D_0 can be obtained by measuring the integrated intensity of a ground-state rotational transition in each of H_2O, HF, and $H_2O\cdots HF$ in an equilibrium mixture containing the three components at a single temperature T (indirectly in the case of HF, as it turns out). The integrated intensities lead, *via* the known rotational partition functions, to the number densities $n_{0,0}(H_2O)$, $n_{0,0}(HF)$, and $n_{0,0}(H_2O\cdots HF)$ of the components in their $v = 0$ and $J = 0$ states and thence, through the simple expression

$$n_{0,0}(H_2O\cdots HF)/n_{0,0}(H_2O)n_{0,0}(HF) = (h^2/2\pi\mu kT)^{\frac{1}{2}} \exp(D_0/RT) \quad (7)$$

to D_0. If sufficient is known about the vibrational frequencies of the dimer (as is the case for $H_2O\cdots HF$), D_0 can be corrected for the zero-point motion to give D_e. The values found[7] for $H_2O\cdots HF$ are $D_0 = 34.3(3)$ kJ mol^{-1} and $D_e = 42.9(8)$ kJ mol^{-1}. As expected, the hydrogen bond in $H_2O\cdots HF$ is relatively strong according to this measure. Although such values of D_0 have not been determined for other members of the series $H_2O\cdots HX$, where X = Cl, CN, or Br, the values of k_σ in Table 5 lead us to expect a decrease in D_0 along the series also. Likewise, if H_2O is replaced by the poorer proton acceptor HCN, we expect the strength of binding to decrease. This is indeed reflected in the smaller values[30,16] $D_0 = 18.45(11)$ kJ mol^{-1} and $k_\sigma = 18.2$Nm^{-1} for $HCN\cdots HF$.

7.2 How Difficult is it to Deform $H_2O\cdots HF$ Angularly?

The ease with which the hydrogen bond in $H_2O\cdots HF$ can be bent is measured by the bending force constants which are available from three main sources: vibrational wavenumbers from infrared spectra, vibrational wavenumbers from satellites in microwave spectra, and vibrational amplitudes from hyperfine structure in microwave spectra. Two coordinate systems have been used in the analysis of results from these experimental methods. The first consists of the angular internal coordinates, as conventionally used in vibrational spectroscopy and defined for the present purpose by θ and ϕ in Figure 10. The second set, the oscillation coordinates as defined by α and β in Figure 10, are conveniently used in the treatment of amplitudes from nuclear quadrupole or nuclear spin–spin hyperfine constants. Transformation between the two coordinate systems allows the combined use of all three types of information when these are available.[31]

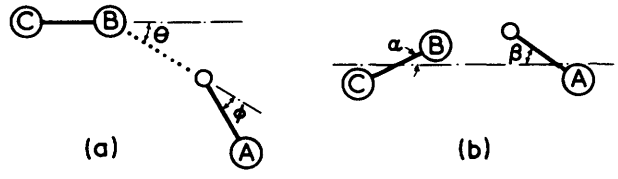

Figure 10 Definition of the oscillation coordinates α and β and the angular internal coordinates θ and ϕ used in the determination of the hydrogen-bond bending force constants of a dimer CB···HA (*e.g.* $H_2O\cdots HF$) from spectroscopic data.

For $H_2O\cdots HF$ all three types of information are in fact available[32,8,2] and this dimer has been treated in more detail than any other member of the series $H_2O\cdots HX$ where there is information only from hyperfine structure at present. The out-of-plane bending potential for $H_2O\cdots HF$ has a double minimum, as already discussed. For in-plane bending the reported force constants[5] are $f_{\theta(i)\theta(i)} = 2.52 \times 10^{-20}$ J rad^{-2} and $f_{\phi(i)\phi(i)} = 19.70 \times 10^{-20}$ J rad^{-2}. It is seen that bending at hydrogen is much more strongly resisted than bending at oxygen. The implication is that distortion of hydrogen bonds at the demand of the environment in condensed phases is energetically more likely to be met by bending at oxygen than at hydrogen. Finally, it is of interest to compare the relative resistance to in-plane bending and out-of-plane bending at oxygen. The former has a single minimum potential while the latter has a double minimum, and not surprisingly it has been shown that the zero-point amplitude of out-of-plane bending is much larger than that for in-plane bending, and correspondingly in-plane distortion is more strongly resisted than out-of-plane distortion. It has been pointed out that if this is generally true for hydrogen bonding to oxygen then it allows an interpretation[5] of an observation from statistical analyses of large numbers of diffraction investigations for hydrogen bonds of the type O···H–O in the solid state. The analyses show that, while there is some preference for hydrogen bonding in the plane containing the axes of the non-bonding pairs on oxygen, there is no favoured angle for hydrogen-bond formation in that plane.[5]

For the remaining members of the series $H_2O\cdots HX$ that have been investigated, information about bending force constants is derived solely from amplitudes of the HX oscillation in the dimer.[33] Values of $k_{\beta\beta}$ that have been obtained are as follows: $H_2O\cdots HF$ 23.8×10^{-20} J rad^{-2}; $H_2O\cdots HCl$ 10.0×10^{-20} J rad^{-2}; $H_2O\cdots HCN$ 5.9×10^{-20} J rad^{-2}. As might be expected they are found to decrease along the series with k_σ.

8 What Electric Charge Redistribution Occurs on Formation of $H_2O\cdots HX$?

When a dimer $H_2O\cdots HX$ is formed by bringing the infinitely separated components together there is inevitably some electric charge rearrangement. This will of course include polarization

of one molecule by the other and *vice versa*. There is also, however, the possibility of transfer of charge, either electronic or protonic, between the two components. The measureable quantities so far available that carry information about charge redistribution are the electric dipole moment enhancement and the various nuclear hyperfine coupling constants of the HX subunit. Arguments based on the H,F nuclear spin – nuclear spin coupling constant in $H_2O\cdots HF$ (see Section 6) indicate that the extention δr of the HF bond within the dimer is small and that proton transfer can be ignored. It is difficult to separate the contributions of electron transfer and polarization to the above-mentioned observable but for $Xe\cdots HCl$ Flygare and coworkers[34] concluded that less than 5×10^{-4} e is transferred from Xe to HCl. Hence, polarization is likely to be the predominant contributor.

The observable quantity that is most directly related to electric charge redistribution on hydrogen bond formation is the electric dipole moment of the dimer. For $H_2O\cdots HF$ more detailed studies have been made than for any other dimer while no information is yet available for any other member of the series $H_2O\cdots HX$. Stark effect measurements in the rotational spectrum of $H_2O\cdots HF$ have led to values of the dipole moment of the dimer, not only in its vibrational ground state but also in excited vibrational states associated with the low-lying intermolecular modes.[3] The results are collected in Table 6 where the nomenclature $[v_{\beta(o)}, v_{\beta(i)}, v_\sigma]$ denotes the vibrational quantum numbers of the three modes illustrated in Figure 1, namely the out-of-plane bending mode $\nu_{\beta(o)}$, the in-plane bending mode $\nu_{\beta(i)}$ and the stretching mode ν_σ, respectively.

The value $\mu = 4.073$ D for the ground state implies an effective enhancement of 0.39 D over the sum of the monomer moments. This enhancement is low by comparison with that of 0.80 D obtained for $HCN\cdots HF$ but it has to be remembered that enhancement reflects not only electronic changes but is also determined in part by zero-point effects. The main contribution to such effects arises from the large amplitude out-of-plane bending mode and when allowance for this is made the enhancement increases to 0.68 D. A correction for the smaller zero-point effects of the other intramolecular modes can also be estimated.

Table 6 Dependence of the electric dipole moment of $H_2O\cdots HF$ on vibrational state

Vibrational state $(v_{\beta(o)}, v_{\beta(i)}, v_\sigma)$	μ/D
(0, 0, 0)	4.073(7)
(1, 0, 0)	3.802(7)
(0, 1, 0)	4.074(16)
(1, 1, 0)	3.76(4)
(0, 0, 1)	3.91(4)

For $\nu_{B(i)}$ and ν_σ the effect of one half quantum of zero-point motion is available from Table 6. The only remaining intermolecular modes to consider are the high frequency bending modes, denoted $\nu_{B(o)}$ and $\nu_{B(i)}$, in which essentially the HF molecule oscillates through the angle β defined in Figure 10. Assuming that, for the purpose of calculating this small correction, the two modes may be considered isotropic and degenerate we can write the reduction as $2\mu_{HF}(1 - \cos\beta_{av})$ in which $\cos\beta_{av}$ is available from amplitude studies described in Section 7. By taking all the intermolecular modes into account, we find the dipole enhancement to be 0.89 D. If we assume that the zero-point effects of all the monomer modes remain unchanged on dimer formation then this enhancement is the value appropriate to planar $H_2O\cdots HF$, *i.e.* to a geometry with $\theta = 0$, by comparison with non-interacting monomers with the same geometric relationship.

More indirect evidence about charge redistribution comes from an interpretation of the Cl-nuclear quadrupole coupling constants in the series of dimers $B\cdots HCl$ (including $B = H_2O$).[35] This interpretation considers the response of the electronic distribution in HCl to the electric charge distribution of B and provides a goal for *ab initio* calculations of charge rearrangement and in particular the consequences close to quadrupolar nuclei.

9 How Much $H_2O\cdots HF$ is Formed in Gas Mixtures of H_2O and HF?

It was indicated in Section 7.1 how spectroscopic measurements on $H_2O\cdots HF$ in an equilibrium mixture with H_2O and HF can give the dissociation energy, D_0, as well as the rotational and vibrational partition functions of the dimer. By taking all this information together it becomes possible to calculate changes in thermodynamic properties for the formation of the dimer from the monomers.[36] This, for $T = 298.15$K, $\Delta H^\ominus_m = -39.1$ kJ mol^{-1}, $\Delta S^\ominus_m = -94.2$ J K^{-1} mol^{-1}, and $\Delta G^\ominus_m = -11.0$ kJ mol^{-1}. Hence we can estimate that for this temperature with initial partial pressures $p_{HF} \approx p_{H_2O} \approx 1$ Torr there is a 10% conversion to $H_2O\cdots HF$, while for initial pressures of 100 mTorr (as typically used in microwave spectroscopy) there is still a 1% conversion. This is much higher than for any other dimer so far investigated. For example, the conversion for $HCN\cdots HF$ under the same spectroscopic conditions is 5×10^{-4}%. No other dimer $H_2O\cdots HX$ has so far been observed spectroscopically in an equilibrium mixture. Evidently, even for $H_2O\cdots HCl$ $\Delta H^\ominus_m$ has too small a magnitude to allow detection with present sensitivity.

10 References

1 J. W. Bevan, A. C. Legon, D. J. Millen, and S. C. Rogers, *J. Chem. Soc., Chem. Commun.*, 1975, 341; J. W. Bevan, Z. Kisiel, A. C. Legon, D. J. Millen, and S. C. Rogers, *Proc. R. Soc. London, Ser. A*, 1980, **372**, 441.
2 Z. Kisiel, A. C. Legon, and D. J. Millen, *Proc. R. Soc. London, Ser A*, 1982, **381**, 419.
3 Z. Kisiel, A. C. Legon, and D. J. Millen, *J. Chem. Phys.*, 1983, **78**, 2910.
4 A. C. Legon and L. C. Willoughby, *Chem. Phys. Lett.*, 1982, **92**, 333.
5 Z. Kisiel, A. C. Legon, and D. J. Millen, *J. Mol. Struct.*, 1984, **112**, 1.
6 Z. Kisiel, A. C. Legon, and D. J. Millen, *J. Mol. Struct.*, 1985, **131**, 201.
7 A. C. Legon, D. J. Millen, and H. M. North, *Chem. Phys. Lett.*, 1987, **135**, 303.
8 A. C. Legon and L. C. Willoughby, *Chem. Phys. Lett.*, 1983, **95**, 449.
9 A. C. Legon and A. P. Suckley, *Chem. Phys. Lett.*, 1988, **150**, 153.
10 A. J. Fillery-Travis, A. C. Legon, and L. C. Willoughby, *Proc. R. Soc. London, Ser. A*, 1984, **396**, 405.
11 G. T. Fraser, K. R. Leopold, and W. Klemperer, *J. Chem. Phys.*, 1983, **80**, 1423.
12 T. R. Dyke, K. M. Mack, and J. S. Muenter, *J. Chem. Phys.*, 1977, **66**, 498.
13 P. Herbine and T. R. Dyke, *J. Chem. Phys.*, 1985, **83**, 3768.
14 H. O. Leung, M. D. Marshall, R. D. Suenram, and F. J. Lovas, *J. Chem. Phys.*, 1989, **90**, 700.
15 D. J. Millen, *Can. J. Chem.*, 1985, **63**, 1477.
16 A. C. Legon and D. J. Millen, *J. Am. Chem. Soc.*, 1987, **109**, 356.
17 A. C. Legon and D. J. Millen, *Discuss. Faraday Soc.*, 1982, **73**, 71.
18 R. A. Collins, A. C. Legon, and D. J. Millen, *J. Mol. Struct.*, 1987, **162**, 31.
19 A. C. Legon and D. J. Millen, *Chem. Soc. Rev.*, 1987, **16**, 467.
20 A. D. Buckingham and P. W. Fowler, *Can. J. Chem.*, 1985, **63**, 2018.
21 A. C. Legon and D. J. Millen, *Can. J. Chem.*, 1989, **67**, 1683.
22 R. J. Gillespie and R. S. Nyholm, *Quart. Rev. Chem. Soc.*, 1957, **11**, 339.
23 R. F. W. Bader, R. J. Gillespie, and P. J. MacDougall, *J. Am. Chem. Soc.*, 1988, **110**, 7329.
24 A. C. Legon and D. J. Millen, *Chem. Phys. Lett.*, 1988, **147**, 484.
25 A. C. Legon and D. J. Millen, *Proc. R. Soc. London, Ser. A*, 1986, **404**, 89.
26 M. M. Szczęsniak, S. Scheiner, and Y. Bouteiller, *J. Chem. Phys.*, 1984, **81**, 5024.
27 A. C. Legon and D. J. Millen, *J. Mol. Struct.*, 1989, **193**, 303.
28 A. C. Legon, C. A. Rego, and A. L. Wallwork, *J. Chem. Phys.* 1990, **92**, 6397.

29 Z. Kisiel, P. W. Fowler, and A. C. Legon, *J. Chem. Phys.*, 1990, **93**, 3054.
30 A. C. Legon, D. J. Millen, P. J. Mjöberg, and S. C. Rogers, *Chem. Phys. Lett.*, 1978, **55**, 157.
31 P. Cope, D. J. Millen, and A. C. Legon, *J. Chem. Soc., Faraday Trans. 2*, 1986, **82**, 1189.
32 R. K. Thomas, *Proc. R. Soc. London, Ser. A*, 1975, **344**, 579.
33 P. Cope, D. J. Millen, and A. C. Legon, *J. Chem. Soc., Faraday Trans. 2*, 1987, **83**, 2163.
34 M. R. Keenan, L. W. Buxton, E. J. Campbell, T. J. Balle, and W. H. Flygare, *J. Chem. Phys.*, 1980, **73**, 3523.
35 A. C. Legon and D. J. Millen, *Proc. R. Soc. London, Ser. A*, 1988, **417**, 21.
36 S. L. A. Adebayo, A. C. Legon, and D. J. Millen, *J. Chem. Soc., Faraday Trans.*, 1991, **87**, 443.